LWT - Food Science and Technology 200 (2024) 116206

Contents lists available at ScienceDirect

LWT

journal homepage: www.elsevier.com/locate/lwt

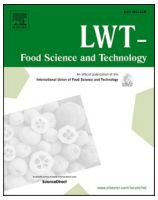

Insights into the enzymatic synthesis of alcoholic flavor esters with molecular docking analysis

Yiran Bian [a,1], Yi Zhang [b,1], Taosuo Wang [a], Chuang Yang [a], Zhiming Feng [c], Kheng-Lim Goh [d], Yibin Zhou [a,**], Mingming Zheng [a,b,*]

[a] Key Laboratory of Jianghuai Agricultural Product Fine Processing and Resource Utilization, Ministry of Agriculture and Rural Affairs, Anhui Engineering Research Center for High Value Utilization of Characteristic Agricultural Products, College of Tea & Food Science and Technology, Anhui Agricultural University, Hefei, 230036, China

[b] Oil Crops Research Institute, Chinese Academy of Agricultural Sciences, Hubei Key Laboratory of Lipid Chemistry and Nutrition, Hubei Hongshan Laboratory, Key Laboratory of Oilseeds Processing, Ministry of Agriculture, Wuhan, 430062, China

[c] Department of Chemical Engineering, Imperial College London, London, SW7 2AZ, UK

[d] Newcastle University in Singapore, 172A Ang Mo Kio Avenue 8 #05-01, 599493, Singapore

ARTICLE INFO

Keywords:
Ethyl caproate
Immobilized lipase
Flavor esters
Green synthesis

ABSTRACT

The enzymatic synthesis is essential for the flavor esters in the food and fragrance industries. This paper introduces a novel preparation method for lipase microarrays (CALB@PMHOS-TEOS) with loadings up to 229 ± 1.4 mg/g. Using surfactant-free hydrophobic silica-hybridized mesoporous materials and *Candida antarctica* lipase, this resulted in the effective synthesis of flavor esters. Using CALB@PMHOS-TEOS a Pickering emulsion system was formed at the oil-water interface for the sustainable synthesis of flavor esters. This resulted in a 93.5 ± 0.5 % conversion of hexanoic acid within 2 h at an optimal temperature of 35 °C, which is the highest level recorded in the literature to date. Furthermore, the conversion of hexanoic acid was maintained at 63.9 ± 1.2 % after 9 cycles of CALB@PMHOS-TEOS reuse. The application of the enzyme to the synthesis in a variety of flavor esters achieved a new benchmark in the existing literature. A molecular docking model was evaluated to understand the molecular mechanism underpinning the immobilized lipase. This work introduces a novel method for the eco-friendly and efficient synthesis of flavor esters for applications across various fields including food and cosmetics.

1. Introduction

Flavor compounds form the fundamental building blocks of both flavors and fragrances and are commonly found in nature. These compounds can evoke pleasing sensations, including fruity, floral, spicy, creamy or nutty aromas (SÁ, Meneses, Araújo, & Oliveira, 2017). Short-chain esters, constituting natural flavor compounds, are frequently used in the food, cosmetic, and pharmaceutical sectors as food additives, antioxidants and surfactants (SÁ et al., 2017; Vasilescu et al., 2019). The global flavors and fragrances market, including blends, essential oils, different natural flavors and fragrance chemicals, has the potential for significant growth. The market is expected to experience a compound annual growth rate (CAGR) of 4.90% during the forecast period spanning from 2019 to 2025 (Bhavsar & Yadav, 2018).

At present, the extraction method for obtaining flavor esters from natural sources does not satisfy the demand. This is due to the low content of flavor substances in plants, resulting in extremely low yield that is not cost-effective (de Barros, Fonseca, Fernandes, Cabral, & Mojovic, 2009). Chemical synthesis involving robust acids or bases as catalysts conducted at elevated temperatures and pressures can enhance production efficiency (Gawas, Lokanath, & Rathod, 2018). However, this method has several drawbacks, notably a lack of natural origin,

* Corresponding author. Key Laboratory of Jianghuai Agricultural Product Fine Processing and Resource Utilization, Ministry of Agriculture and Rural Affairs, Anhui Engineering Research Center for High Value Utilization of Characteristic Agricultural Products, College of Tea & Food Science and Technology, Anhui Agricultural University, Hefei, 230036, China.

** Corresponding author.

E-mail addresses: zhouyibin@ahau.edu.cn (Y. Zhou), zhengmingming@caas.cn (M. Zheng).

[1] Both authors contributed equally to this paper.

https://doi.org/10.1016/j.lwt.2024.116206
Received 18 January 2024; Received in revised form 6 May 2024; Accepted 11 May 2024
Available online 12 May 2024

challenging manufacturing requirements, low product purity, difficulties in raw material recovery, numerous side reactions, and significant environmental pollution concerns (Jaiswal & Rathod, 2022). Hence, the bioenzyme-catalyzed method was selected for the synthesis study. Enzymatically synthesized flavor esters can be produced under mild conditions with minimal energy input and pollutant emissions, thus meeting the requirements of green and sustainable production (Chen et al., 2023). Within the enzyme family, lipase stands out as an enzyme capable of catalyzing a wide range of reactions including hydrolysis, acidification, esterification and ester exchange across various media, such as organic solvents, ionic liquids, supercritical fluids, etc. (Elgharbawy, Riyadi, Alam, & Moniruzzaman, 2018; Ghanem & Aboul-Enein, 2004; Kumar, Dhar, Kanwar, & Arora, 2016). Lipase exhibits remarkable chemoselectivity, regioselectivity and stereoselectivity, rendering it a versatile tool that is extensively used in the synthesis of flavor esters (Monteiro et al., 2019). Several enzyme immobilization techniques have been developed to address the problems of unstable activity and poor reusability connected with free enzymes, including physical methods, such as adsorption (Lammirato, Miltner, & Kaestner, 2011) and embedding (Bai & Wu, 2022), as well as chemical methods, such as covalent attachment (Al-Lolage, Meneghello, Ma, Ludwig, & Bartlett, 2017) and cross-linking (Naseer et al., 2020), have been developed. Previous studies indicated that chemical methods could be expensive and could have a low recovery rate. Therefore, physical methods are predominantly used for immobilization.

Appropriate carriers can enhance the stability and catalytic performance of enzymes under specific conditions by providing a protective effect. Among the diverse array of immobilized carriers, mesoporous materials stand out as solid materials with pores ranging from 2 to 50 nm. They offer advantages such as adequate pore size distribution, a considerable specific surface area, customizable pore size, strong stability, and promising development prospects (L. Wang, Ding, & Sun, 2016). However, surfactants have traditionally played a crucial role in the preparation of these mesoporous materials. It is important to note that surfactants can be costly, and its use could have a negative impact on the environment (Yang et al., 2007). Hence, non-templated hybrid SiO_2 is synthesized without the addition of surfactants or other reagents with structure-directed properties, for the preparation of immobilized lipases.

The Pickering emulsion system serves as an effective and stable reaction system. The biphasic reaction system involves solid particles arranged closely at the oil-water interface. The arrangement minimizes enzyme inhibition by substrates and products, improves the enzyme stability, and simplifies enzyme recycling (Jiang, Li, Hong, & Ngai, 2018; Z. Wang, van Oers, Rutjes, & van Hest, 2012). In Pickering emulsions, the droplet size typically falls within the micron range, thereby increasing the interface area between the aqueous phase and the organic medium in the two-phase system. This promotes mass transfer and enhances catalytic efficiency (Jiang et al., 2018). Many studies have utilized appropriately sized carriers to create Pickering emulsions. Wang and co-workers utilized a co-solvent method to synthesize poly (ethylene glycol)-b-poly (styrene-3-isopropenyl-a, a-dimethylbenzyl isocyanate) polymer, creating a biphasic enzyme-catalyzed stable Pickering emulsion system. They successfully loaded the CALB enzyme into the lumen of the polymer, resulting in significant enhancement of the catalytic performance (Z. Wang et al., 2012). In a previous study conducted in the laboratory, the mesoporous carbon spheres (MCS) were prepared. These MCS were utilized to stabilize the preparation of the Pickering emulsion system and were subsequently employed in the reaction, resulting in a significant enhancement in the conversion rate (Dong et al., 2019). This provides a new approach for achieving the stable and efficient synthesis of flavor esters.

In this study, the surfactant-free organic-inorganic silica oxide hybrid mesoporous materials were first synthesized and then prepared immobilized lipase microarrays (CALB@PMHOS-TEOS) by immobilizing lipase CALB within these materials. The conditions affecting lipase immobilization were systematically investigated. By employing hydrophobic immobilized enzyme as both emulsifier and catalyst, the flavored esters were efficiently prepared in a Pickering emulsion enzyme system. The effects of water content, enzyme addition, substrate molar ratio and esterification temperature on the synthesis of ethyl caproate were investigated. The reusability, wide applicability and stability of the immobilized lipase microarrays were demonstrated. To the best of the knowledge, this is the first study on sustainable flavor ester synthesis in a Pickering emulsion system using organic-inorganic silica oxide hybrid mesoporous material. The findings reported this is important for environmentally friendly flavor ester synthesis with potential application in the food and cosmetics sectors.

2. Materials and methods

2.1. Materials

Hexanoic acid (99%), n-octanoic acid (99%), n-heptanoic acid (98%), tetraethyl silicate (99%) and polymethyl hydrogenated siloxane (PMHS, viscosity = 15–40 mPa s at 20 °C) were purchased from Aladdin Biotech, Ltd. (Shanghai, China). Nonanoic acid (98%) and lauric acid (98%) were obtained from Maclean Biochemical Technology Co., Ltd. (Shanghai, China). Decanoic acid, anhydrous ethanol, and n-hexane were purchased from Sinopharm Chemical Reagent Co. Ltd. N-Pentanoic acid was bought from Titan Technology Co., Ltd. (Shanghai, China). NaOH was purchased from Xilong Technology Co. Ltd. Lipase CALB (*Candida antarctica* lipase B) was purchased from Novozymes (Beijing, China). Enhanced (BCA) Protein Assay Kit was obtained from Shanghai Yuan Ye biotechnology. P-nitrophenyl palmitate (p-NPP) was purchased from Sigma-Aldrich (St Louis, USA). All reagents and solvents used in the experiments were of analytical and chromatographic grade.

2.2. Preparation of non-template hybridized SiO_2 carriers

The hybridized mesoporous silica was prepared following the method reported by Yang et al. (2007). Polymethyl hydrogen-containing siloxane (PMHS) at 0.47 mL was added dropwise to a beaker containing 70 mL of anhydrous ethanol and 50 mg of NaOH, and stirred vigorously for 24 h. The previously described mixture was then agitated for 1 h while a small amount of deionized water was added. Subsequently, 5 mL of tetraethyl silicate (TEOS) was added, followed by 3 h of stirring and static aging period of 48 h to obtain the gel. Finally, the gel was subjected to drying in an oven (DHG-9140 A, Yi Heng, China) at 60 °C for 24 h to eliminate any residual ethanol. It was then milled to yield the non-templated hybridized SiO_2 carriers (PMHOS-TEOS), which is a porous material incorporating methyl organic-inorganic silicon oxide.

2.3. Immobilization of lipase on PMHOS-TEOS and reusability study

In this work, CALB@PMHOS-TEOS was created by immobilizing the commercial lipase CALB on the PMHOS-TEOS carrier, following the method reported by Chen et al. with certain modifications (Chen et al., 2023). To acquire the required concentration of lipase solution, 10–50 mg of lipase CALB was dispersed in 1 mL of phosphate buffer (PBS, 50 mmol/L, pH = 7) and stirred at 200 rpm for 5 min at 4 °C. Next, 0.1 g of PMHOS-TEOS (using 200 μL ethanol presoaked) was added to 3–15 mL of lipase solution, followed by a 5 min of ultrasonic treatment (YM-060 S, Fang'ao Microelectronics, China) and 5 min of vacuum treatment (SHZ-DIII, Si Tai, China). Subsequently, the mixture was centrifuged for 10 min at 8000 rpm after oscillating it for 40 min at 30 °C at a speed of 220 rpm. The supernatant was collected to assess the residual protein content and the sediment (CALB@PMHOS-TEOS) using the BCA protein detection technique. The sediment was washed using phosphate buffer three times, and then freeze-dried overnight.

The amount of remaining protein in the lipase solution was determined by:

$$\text{Loading amount (mg / g)} = \frac{(C_0 - C)V}{M} \quad (1)$$

where C_0 and C are the protein concentrations (mg/mL) before and after immobilization, V is the volume (mL) of the aqueous solution, and M is the mass (g) of the PMHOS-TEOS.

To investigate the reusability, the immobilized enzyme was collected via centrifugation at the end of the experiment. It was then subjected to three washes with n-hexane, followed by vacuum drying, allowing for its reuse in the subsequent reaction batch.

2.4. Characterization of PMHOS-TEOS and CALB@PMHOS-TEOS

The surface morphologies of PMHOS-TEOS were characterized using a scanning electron microscope (SEM; Hitachi S-4800; Japan) and the electron beam voltage was set at 200 kV. A small amount of PMHOS-TEOS powder was bonded with conductive adhesive tape, and the poorly bonded powder was removed by tapping for SEM characterization. A computer-controlled nitrogen gas adsorption analyzer (ASAP 2010; USA) was used to measure the total pore volume and the Brunauer—Emmett-Teller (BET) surface area within a relative pressure range of 0.05–1.00. To analyze the characteristic absorption peaks of PMHOS-TEOS and CALB@PMHOS-TEO, the materials were first combined with KBr, pulverized with a mortar, dried under a baking lamp (ZHD-10; China) and finally examined using an FT-IR spectrometer (Nicolet iS50; USA). A contact angle goniometer (SINDIN, SDC-200 S; China) was used to measure the water contact angles of PMHOS-TEOS. Data from X-ray photoelectron spectroscopy (XPS) was gathered using the ESCALAB 250 XI device. Using a Nikon A1 confocal microscope, fluorescence confocal laser scanning microscopy (CLSM) pictures were taken.

2.5. Enzymatic synthesis of ethyl caproate

Hexanoic acid was esterified with anhydrous ethanol to produce ethyl hexanoate by an enzymatic process (Musa, Latip, Abd Rahman, Salleh, & Mohamad Ali, 2018). A 5 mL vial was filled with hexanoic acid and anhydrous ethanol (molar ratio of acid to ethanol ranging from 1:1 to 1:5). Deionized water (18.9 wt%-53.8 wt%) and corresponding lipases (1%–5% of substrate mass) were then added. Vibrant shearing at 20 000 rpm for 1 min produced a stable Pickering emulsion. The mixture was then placed in a water bath (35 °C, 200 rpm) for 2 h of reaction. In enzymatic esterification processes, 20 μL of reacted solution was sampled at an interval of 15 min and diluted with n-hexane to 50 times. The collected samples were subjected to high performance gas chromatography analysis after being filtered with a 0.22 μm PDVF filter. Finally, the immobilized lipases were gathered by centrifugation, laundered with n-hexane and dried for subsequent reaction cycles.

2.6. GC analysis of ethyl caproate

The yield of ethyl hexanoate in the reaction mixture was evaluated following the procedure suggested by Han. et al. (2009) with appropriate modifications. The conversion rate of ethyl hexanoate was analyzed using a gas chromatograph (7890 A, Agilent; USA) featuring a hydrogen flame ionization detector and a fused silica capillary column (DB-FastFAME, 0.25 mm × 30 m × 0.25 μm, Agilent Technologies). The carrier gas used was nitrogen, with a total gas flow rate was 21 mL/min. The temperature of the injector and detector were controlled at 275 °C and 250 °C, respectively. The oven program was started at 80 °C for 1 min and then ramped up at 10 °C/min to 170 °C for 5 min. The shunt ratio was 20:1.

2.7. Determination of thermal stability of immobilized enzymes

Thermal stability was evaluated by measuring the generation of p-nitrophenol through the hydrolysis of free and immobilized CALB when exposed to varying temperatures during the reaction with p-nitrophenyl palmitate (p-NPP) (Zhang et al., 2022; Zheng, Zhu, et al., 2015). Twenty mg of free or immobilized enzyme was added to 1 mL of PBS (50 mmol/L, pH = 7.00). Next, the mixture was subjected to heating in water at a specificized temperature range (55–95 °C) for 120 min, followed by cooling to room temperature. Thereafter, 1 mL of 0.5% p-NPP/EtOH solution (w/v) was blended into the mixture by stirring at 180 rpm for 5 min at 37 °C. The reaction was initiated by adding 2 mL of 0.5 mol/L Na_2CO_3 and then centrifuged for 10 min (10 000 rpm). The 1 mL of supernatant was diluted 10-fold with distilled water and the remaining lipase activity was assessed at 410 nm using a UV/VIS spectrophotometer (Beckman DU-800, Fullerton; USA). Relative activity, which is computed as the ratio of the surviving activity to the activity before the heat incubation using the following formula, was used to evaluate the thermal activity of the immobilized enzyme:

$$\text{Enzyme activity (nkat / g)} = = \frac{A \times V \times N \times 10^3}{\varepsilon_{410} \times t \times M} \times 16.67 \quad (2)$$

where M is the mass of free or immobilized enzyme (g), N is the dilution multiple, A is the absorbance measured at 410 nm, V is the total volume after dilution (mL), t is the hydrolysis reaction time (min), ε_{410} is the molar absorbance coefficient of p-NPP (14.298×10^3 $M^{-1}cm^{-1}$).

2.8. Molecular docking analysis

A molecular docking model was developed to evaluate the interaction between lipase and fatty acids, using AutoDock Tools 1.5.6. The free CALB crystal structure (PDB: 1TCA) was derived from the Protein Data Bank (Zhang et al., 2022). The 3D structures of fatty acids were derived from PubChem. The conformations with the lowest docking energies were selected as the primary conformations of the fatty acids using Lamarckian GA as the docking algorithm. The molecular docking method was modified appropriately based on the method reported by Qin, Zhong, and Wang (2021). The procedure was as follows. First, the hydrogenation of proteins in AutoDock was selected as the receptors. Next, small molecules were designated as ligands for hydrogen bonding and subjected to force field optimization. Subsequently, docking parameters and a docking box were configured to encompass both the protein and small molecules. Subsequently, AutoDock Vina was used to identify the conformation with the lowest docking energy, which was considered as the complex output. Finally, the docking model was visualized and analyzed using PyMOL software to calculate the binding energy.

3. Results and discussion

3.1. Reaction systems

It is well-established that lipases can be activated at the oil-water interface. Therefore, the presence of water and its effect on the catalytic efficiency of lipases play a crucial role in ester formation (Kuang, Zhang, Li, & Tian, 2020). The conversion percentage of ethyl hexanoate catalyzed by both the free enzyme (CALB) and immobilized enzyme (CALB@PMHOS-TEOS) in both single-phase and biphasic systems is illustrated in Fig. 1. The conversion percentages of the free enzyme were 99.9 % and 8 ± 0.2 % for 2 h of reaction with and without water respectively. The conversion percentages for the immobilized enzyme were 88.4 ± 0.7 % and 83.2 ± 0.6 % for 2 h of reaction with and without water, respectively. Free lipase exhibits slow and relatively low reactivity in the CALB single-phase system. However, the reactivity increases in the presence of added water, which facilitates the interaction between the enzyme and the substrate, promoting the formation of the target product (Luan & Zhou, 2017). The conversion percentage of the immobilized enzyme in the presence of water is 5.2% higher than that in the single-phase system, reinforcing argument that lipases can facilitate

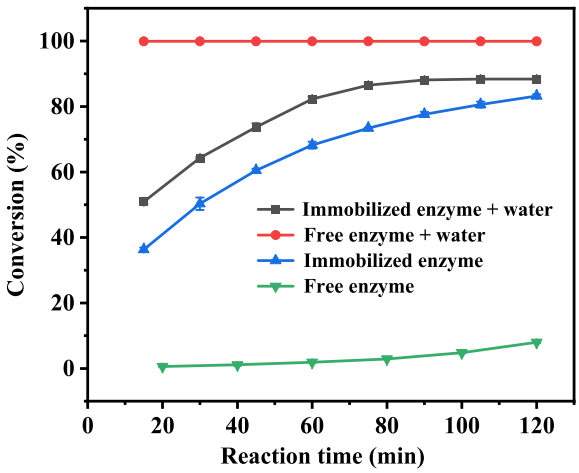

Fig. 1. Graph of conversion percentage versus reaction time corresponding to different treatment of free and immobilized enzymes. The reaction was carried out in deionized water (1 mL), n-hexanoic acid (1.26 mL), anhydrous ethanol (1.17 mL) and enzyme (40 mg) in a water bath (35 °C, 200 rpm) for 2 h. The results presented here was used for screening of reaction systems for the enzymatic synthesis of ethyl hexanoate.

the reaction at the oil-water interface. The results in Fig. 1 illustrate that the immobilized enzyme in the two-phase system exhibits a lower reaction rate compared to the free enzyme. This difference can be attributed to structural and conformational changes in the enzyme following immobilization. These changes alter the active center, increase spatial and internal diffusion resistance, and can lead to partial enzyme inactivation and reduced enzyme viability (H. Wang, Zhang, Yue, Liang, & Su, 2022). Hence, this paper investigates the synthesis of flavor esters through the preparation of immobilized enzymes in a biphasic system.

3.2. Characterization of PMHOS-TEOS and CALB@PMHOS-TEOS

Scanning electron microscopy (SEM) was used to characterize the surface morphology of PMHOS-TEOS. As indicated in Fig. 2a, PMHOS-TEOS exhibited irregular, stone-like particles of different sizes. Fig. 2b shows the wormhole-like mesoporous channels, which are formed by the nano-phase separation associated with the formation of non-surfactant aggregate interactions with inorganic silica matrix during the sol-gel process, due to the addition of TEOS in the preparation conditions, from which silica spheres are also evident (Nagappan, Lee, Seo, Park, & Ha, 2015; Yang et al., 2007). As shown in Fig. 2c, the nitrogen adsorption-desorption isotherms show typical type IV and H1 isotherm patterns, thus revealing its mesoporous structure with a pore size of about 10 nm for PMHOS-TEOS, which facilitates the entry of lipase CALB into the PMHOS-TEOS cavity (Xu, Yang, Wang, Huang, & Zheng, 2021; Yang et al., 2007).

To verify the successful immobilization of the lipase CALB on PMHOS-TEOS, Fourier transform infrared spectroscopy (FT-IR) was used to characterize the structure of the material and the immobilized lipase. Fig. 2d shows the IR spectra of the carrier, enzyme and immobilized enzyme. The peak at 2980 cm^{-1} in the carrier PMHOS-TEOS corresponded to the stretching vibration of C–H in the methyl group. Furthermore, the stretching and bending vibrations of the *Si*–C bond were identified as the source of the absorption peaks at 1275 cm^{-1} and 775 cm^{-1}, respectively (Pélisson et al., 2017; Zhai, Song, Zhai, An, & Ha, 2012; Çıtak, Erdem, Erdem, & Öksüzoğlu, 2012). In addition to the characteristic peaks of the carriers on 2980 cm^{-1}, 1275 cm^{-1} and 775 cm^{-1}, free CALB and CALB@PMHOS-TEOS have the same adsorption bands in the 1535 cm^{-1} region. The bands show a correlation with the N–H bond's bending vibration, indicating that lipase CALB was successfully loaded onto the carriers (Sun, Dong, Wang, Huang, & Zheng, 2020; Zheng, Mao, et al., 2015).

X-ray photoelectron spectroscopy (XPS) measurements of PMHOS-TEOS and CALB@PMHOS-TEOS surface element compositions further demonstrated the successful loading of the lipase CALB on the carrier PMHOS-TEOS. As shown in Fig. 2e&f, the peaks of elements C 1s, Si 2p, O 1s and N 1s corresponded to the following energies, 285.1, 102.1, 532.1 and 399.1 eV, respectively. As anticipated, no peaks corresponding to the N element were observed in the PMHOS-TEOS. However, with the CALB@PMHOS-TEOS, the peak corresponding to the N element yielded an increase in the content of 4.96% was observed due to the presence of amino groups in immobilized lipases, confirming the immobilization of lipases (Chen et al., 2023; Lai et al., 2023; Nagappan & Ha, 2017).

The hydrophilicity and hydrophobicity of PMHOS-TEOS were characterized using a contact angle measurement instrument (SDC-200 S). As shown in Fig. S1, the contact angle measures 106°, indicating a high hydrophobicity. This property provides the basis for the formation of the Pickering emulsion interface.

An efficient Pickering emulsion system allows for efficient catalysis by allowing reactant molecules to diffuse automatically (Dong et al., 2019). The laser confocal images of the carrier (Fig. 2g&h) reveal an oil-in-water emulsion system with uniform size and stable loading of the carrier on the surface. Consequently, this significantly improves the oil-water contact and boosts the reaction system's stability.

3.3. Optimization of lipase immobilization condition

3.3.1. Enzyme concentration

It has been shown that raising the protein content may lead to an increase in lipase loading and an improvement in catalytic efficiency. Here, reaction solutions containing 1–5 mg/mL of protein were made, and their effects on the immobilization of lipase were examined. As shown in Fig. 3a, the enzyme loading steadily increased with increasing protein concentration. The initial protein concentration of 3 mg/mL yielded a protein amount in the particle of 195 ± 0.7 mg/g, corresponding to a caproic acid conversion percentage of 92.7 ± 3.8 %. This conversion percentage remained unchanged thereafter with increasing protein concentration. The reason for this is that overproduction of lipase may result in aggregation or multilayer adsorption, which would prevent the substrate from reaching the lipase's active site (Xu et al., 2021). Because it corresponds to the lowest protein concentration beyond which the conversion percentage plateaus, a starting protein concentration of 3 mg/mL was selected for immobilization.

3.3.2. Enzyme solution addition

The control of enzyme adsorption is crucial for the successful preparation of immobilized enzymes (Zheng, Zhu, et al., 2015). To study the impact of lipase solution addition on both the solid loading and catalytic efficiency of the immobilized enzyme, the protein amount in particle and the conversion percentage versus were plotted against the enzyme content in the solution (see Fig. 3b). The range of 3–15 mL lipase solution with an initial protein concentration of 3 mg/mL was added to 0.1 g of the carrier (PMHOS-TEOS). The solid loading (i.e., protein amount in particle) gradually increased with increasing volume of the enzyme solution. The solid loading was 229 ± 9.2 mg/g at the enzyme solution volume of 10 mL; the conversion percentage of hexanoic acid appeared to have plateaued. However, the conversion percentage decreased to 84.5 ± 1.3 % as the solid loading amount increased to 280.5 ± 8.5 mg/g with 15 mL of enzyme solution. This phenomenon arises due to the high lipase content within the carrier, which introduces mass transfer limitations, leading to decreased activity and impeding the adsorption between the carrier and the lipase (Xu et al., 2021; Zheng, Zhu, et al., 2015). Based on the results of solid loading and reaction conversion rate, a lipase solution addition of 10 mL was determined to be the optimal condition.

In summary, the optimal conditions for the preparation of

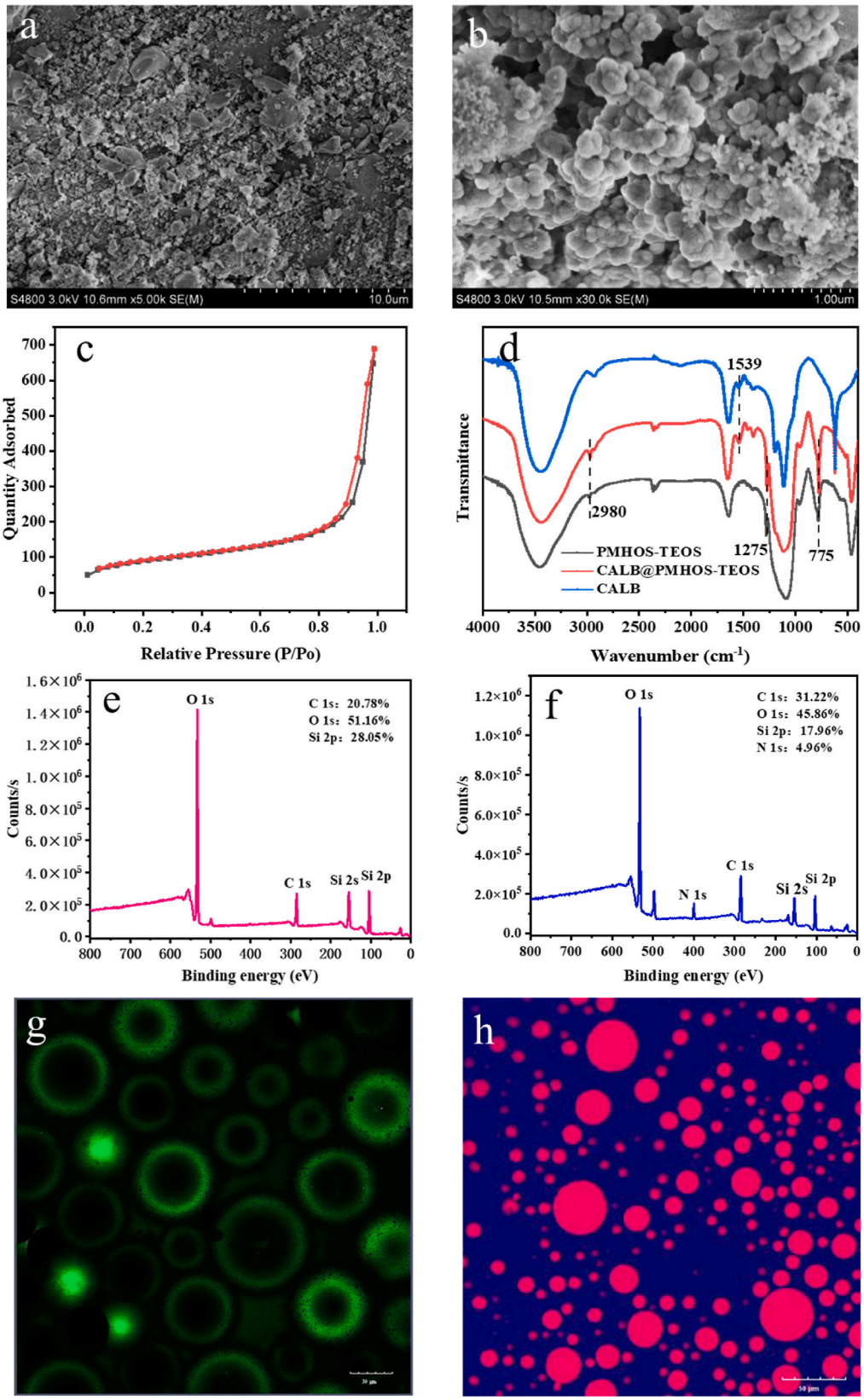

Fig. 2. Characteristics of PMHOS-TEOS. SEM images of PMHOS-TEOS at (a) x5 and (b) x30 magnification. (c) Graph of Quantity Absorbed versus Relative Pressure to illustrate N_2 adsorption-desorption isotherms. (d) Graph of Transmittance versus Wavenumber to illustrate the respective FT-IR spectra of CALB, PMHOS-TEOS and CALB@PMHOS-TEOS. Graphs of Counts versus Binding Energy to illustrate the XPS results of (e) PMHOS-TEOS and (f) CALB@PMHOS-TEOS. CLSM images of Pickering emulsion corresponding to (g) CALB@PMHOS-TEOS stained with FITC-I, and (h) aqueous and oil phases stained with Nile Blue and Nile Red respectively.

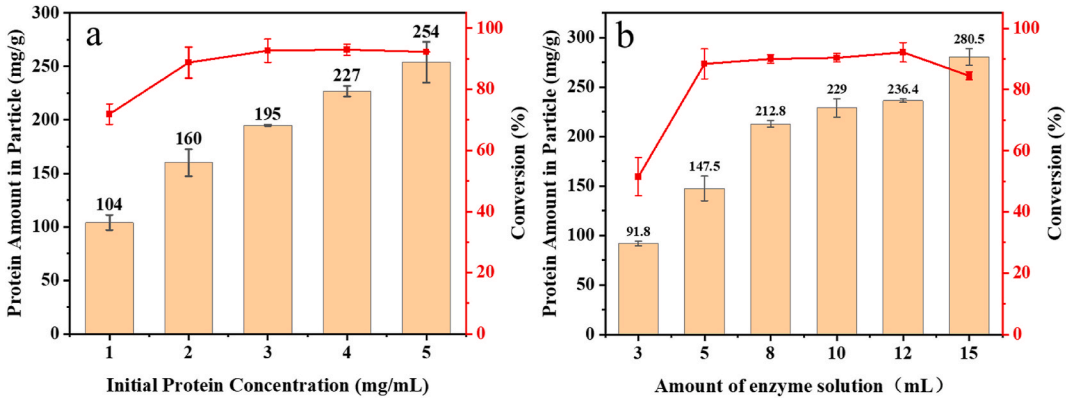

Fig. 3. Graphs of Protein Amount in Particle versus (a) Initial Protein Concentration and (b) Amount of Enzyme Solution to illustrate the effects on immobilized CALB. The reaction was carried out in deionized water (1 mL), n-hexanoic acid (1.26 mL), anhydrous ethanol (1.17 mL) and enzyme (40 mg) in a water bath (35 °C, 200 rpm) for 2 h.

immobilized enzyme corresponded to an initial protein concentration of 3 mg/mL and 10 mL of lipase solution.

3.4. Optimization of reaction conditions

The catalytic effectiveness of lipase and the enzymatic production of ethyl caproate are influenced by the reaction circumstances. This section outlines the influence of various reaction conditions on the conversion percentage. These conditions include water content, enzyme amount, molar ratio of hexanoic acid to ethanol and reaction temperature.

3.4.1. Water content

Fig. 4a shows the effects of water content in the system on the synthesis of ethyl caproate. The conversion percentage increases non-

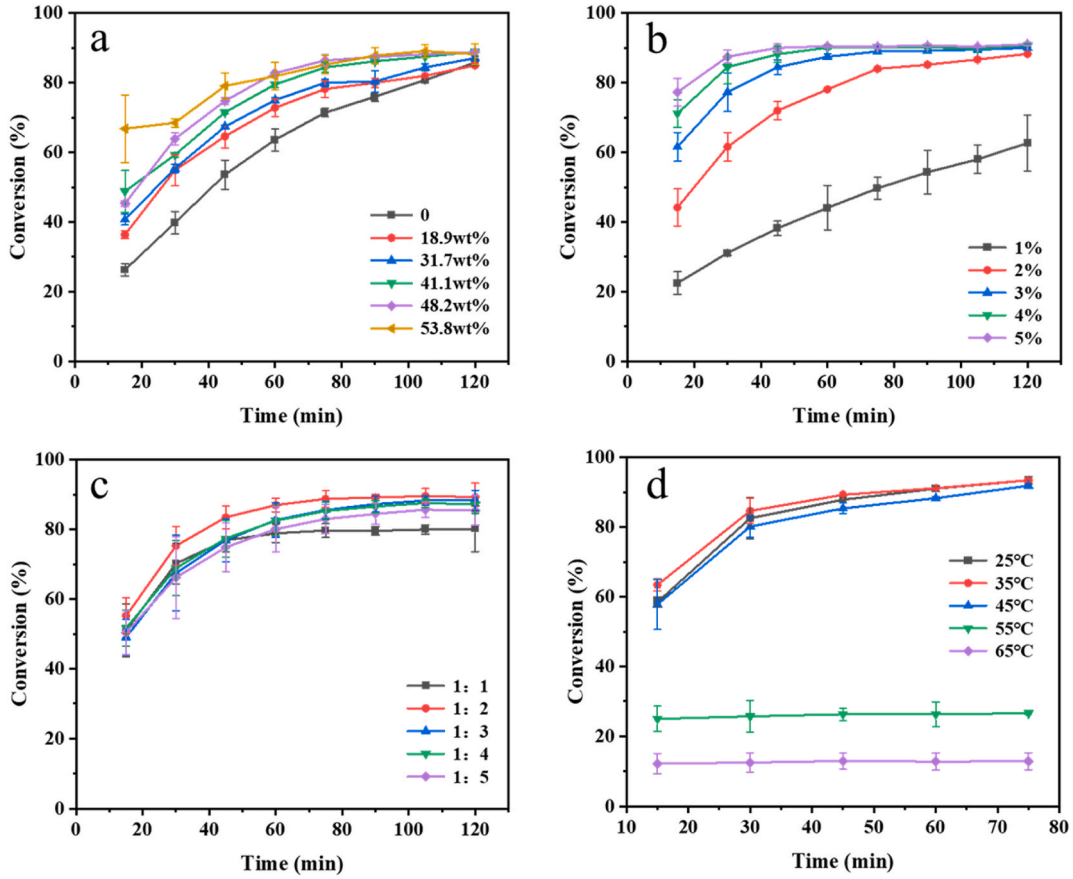

Fig. 4. Graphs of Conversion percentage versus time to illustrate the effects of (a) water content on the synthesis of ethyl hexanoate, (b) enzyme amount on the synthesis of ethyl hexanoate, (c) substrate concentration on the synthesis of ethyl hexanoate and (d) temperature on the synthesis of ethyl hexanoate. In (a), the reactions were carried out in a water bath (35 °C, 200 rpm) in deionized water (18.9 wt%-53.8 wt%), enzyme (2%), and molar ratio of n-hexanoic acid to anhydrous ethanol (1:2) for 2 h. In (b), the reaction was carried out in a water bath (35 °C, 200 rpm) with deionized water (41.1 wt%), enzyme (1%–5%), and a molar ratio of n-hexanoic acid to anhydrous ethanol (1:2) for 2 h. In (c), the reaction was carried out in a water bath (35 °C, 200 rpm) in a molar ratio (1:1–1:5) of deionized water (41.1 wt%), enzyme (3%), n-hexanoic acid and anhydrous ethanol for 2 h. In (d), the reaction was carried out in a water bath (25 °C–65 °C, 200 rpm) with deionized water (41.1 wt%), enzyme (3%), and a molar ratio of n-hexanoic acid to anhydrous ethanol (1:2) for 2 h.

linearly with time; the increase was rapid at the initial stage, i.e., during the period from 20 to 60 min. Subsequently, the conversion percentage curves of the respective water content appeared to converge with increasing time. The conversion percentage ranged from 85 ± 0.5 % to 88.9 ± 0.1 % at time 120 min. The higher the water content, the higher the conversion percentage of the hexanoic acid (at any given time). The maximum value of 88.9 ± 0.1 % at time 120 min was achieved at a water content of 41.1 wt%. This indicates that controlling the quantity of water phase beneath a certain amount of oil phase is crucial for the formation of a stable and effective Pickering emulsion reaction system. An insufficient oil-water contact may arise from an insufficient water phase (Dong et al., 2019). Conversely, a larger water phase increases both the oil-water interface and enzyme-substrate contact. Therefore, a water content of 41.1 wt% was selected for the subsequent reaction.

3.4.2. Enzyme addition

The quantity of enzyme used in any biocatalytic process is crucial, particularly when it comes to large-scale manufacturing. To make it easier to determine the minimal quantity needed to get excellent yields, Fig. 4b illustrates the effects of different enzyme amounts on the reaction in the same reaction system. Similar to the water content effects, the conversion percentage increases non-linearly with time. Apart from the enzyme amount at 1%, the conversion percentage curves of the enzyme content (from 2% to 5%) appeared to converge with increasing time from 20 to 120 min. The higher the enzyme amount, the higher the conversion percentage of the hexanoic acid (at any given time). The maximum value of 90 ± 0.1 % at time 120 min was achieved at an enzyme amount of 3%. However, the convergence of the conversion percentage to around 90% over time suggests that introducing a higher enzyme amount may not lead to a significant further enhancement in the conversion percentage. This observation is consistent with findings reported elsewhere (Foresti & Ferreira, 2005; Musa et al., 2018). This may be due to the agglomeration of immobilized enzyme, as higher catalyst loading may destroy the solubility of the enzyme (Bansode & Rathod, 2014). Therefore, 3% enzyme amount was identified as the minimal level for the optimal conversion to synthesize ethyl hexanoate.

3.4.3. Substrate molar ratio

Fig. 4c illustrates the effects of substrate molar ratio on the conversion of the reaction. Similar to the water content and enzyme amount effects, the conversion percentage increases non-linearly with time; the increase was rapid at the initial stage, i.e., during the period from 20 to 60 min, but gradual at later times. While a change in substrate molar ratio from 1:1 to 1:2 resulted in a large increase in conversion percentage throughout the time from 20 to 120 min (notably conversion percentage of hexanoic acid increased from 80.2 ± 6.6 % to 89.3 ± 4.0 % at time 120 min). The conversion gradually decreased to 85.5 ± 4.2 % when the alcohol-acid molar ratio went from 1:3 to 1:5 (NB: need to see the plot Fig. 4c). This outcome might be the result of the medium's polarity being affected by a rise in acid or alcohol content. The accumulation of polar substrates within the enzyme's aqueous microenvironment alters the solvent's affinity, resulting in reduced conversion (Alvarez-Macarie & Baratti, 2000; Hari Krishna, Divakar, Prapulla, & Karanth, 2001; Laane, Boeren, Vos, & Veeger, 2009; Romero, Calvo, Alba, Daneshfar, & Ghaziaskar, 2005). Additionally, high alcohol concentration acts as a terminal inhibitor of lipase, leading to a decrease the enzyme activity (Badgujar & Bhanage, 2014; Bansode & Rathod, 2014; Jaiswal & Rathod, 2018). Therefore, an acid to alcohol molar ratio of 1:2 was used to achieve optimal ester conversion.

3.4.4. Reaction temperature

Variations in reaction temperature affect both enzyme activity and stability, consequently influencing the reaction rate. Fig. 4d illustrates how the enzymatic production of ethyl hexanoate is affected by temperature changes during the process (25 °C–65 °C). Similar to the previous three conditions, the conversion percentage increases non-linearly with time. Overall, there is little change in the conversion percentage with increasing reaction temperatures from 25 to 35 °C. However, beyond 35 °C the conversion percentage decreases dramatically with increasing reaction temperature. The conversion percentage peaked at 93.5 ± 0.5 % at 75 min, within the temperatures 25 °C–35 °C. Based on the thermal stability study presented below (Table S1), it is evident that lipases maintain their catalytic efficiency better at relatively low temperatures. This suggests that a reaction temperature of 35 °C is more suitable for ethyl hexanoate synthesis. Another important factor is that higher temperatures may lead to the volatilization of alcoholic flavor substances, noticeable during this experiment, which in turn results in lower conversion rates of ethyl hexanoate. Based on the results, it is concluded that the optimal reaction temperature for the enzymatic synthesis of alcoholic flavor esters, such as ethyl hexanoate, is 35 °C.

3.5. Reusability and thermal stability

3.5.1. Reusability of CALB@PMHOS-TEOS

The reusability of immobilized enzymes is important in industrial applications. The stability and potential for long-term utilization of the immobilized enzyme CALB@PMHOS-TEOS were evaluated by assessing its reusability via the cyclic synthesis of ethyl hexanoate. The findings showed a progressive decline in hexanoic acid conversion as the number of CALB@PMHOS-TEOS enzyme reuse cycles increased (Fig. 5a). Over the first 5 cycles, the conversion of hexanoic acid decreased from 90.6 ± 0.6 % to 86.4 ± 0.4%, reflecting a modest 4.2% decrease. After 9 cycles of repeated use, the conversion remained above 60%, indicating no significant degradation in the lipase catalytic efficiency. Unlike the non-recyclable and non-reusable nature of the free enzyme CALB, CALB@PMHOS-TEOS offers increased reusability and cost savings. This is attributed to the presence of PMHOS-TEOS carrier-mediated pore channels, where the enzyme is adsorbed on the inner side of the pore channel. This prevents lipase leakage, reduces shear stress, and enhances overall stability, maintaining catalytic efficiency (Chen et al., 2023).

3.5.2. Thermal stability

The thermal stability of free and immobilized CALB was evaluated by the detection of p-nitrophenol produced by the hydrolysis of p-nitrophenyl palmitate (p-NPP) with varying temperatures ranging from 55 °C to 95 °C. The initial enzyme activities of both free and immobilized enzymes yielded values of 761.8 ± 3.3 nkat/g and 758.5 ± 1.7 nkat/g, respectively, showing little difference (Table S1). However, the activity of free enzyme decreased greatly after incubation, with the relative activity dropping to 11.2 ± 0.5 % at 55 °C and to 7.4 ± 0.1 % at 95 °C (Fig. 5b), indicating a substantial loss of activity. In contrast, the immobilized enzyme showed a gradual decline after incubation with its relative activity remaining at 44.1 ± 0.4% even at 95 °C. The enhanced thermal stability underscores the advantages of enzyme immobilization. According to the study reported by Xu, this is attributed to the formation of hydroxyl groups on the carrier forms and the protein. Through this contact, the lipase's structure is further stabilized, limiting the substantial conformational changes that come with heat denaturation (Xu et al., 2021).

In summary, the reusable enzyme CALB@PMHOS-TEOS catalyzed the synthesis of ethyl hexanoate, resulting in high yield and good thermal stability. The promise of lipase immobilization for industrial applications is shown by the enzyme's reusability and thermal stability.

3.6. Applicability of CALB@PMHOS-TEOS

By examining the catalytic esterification reaction of ethanol with different acids to create different alcoholic taste esters, the wide application of CALB@PMHOS-TEOS was explored (Fig. S2). Table 1 lists the synthesis of various flavor esters, notably ethyl valerate, ethyl hexanoate, ethyl heptanoate, ethyl octanoate, ethyl nonanoate, ethyl

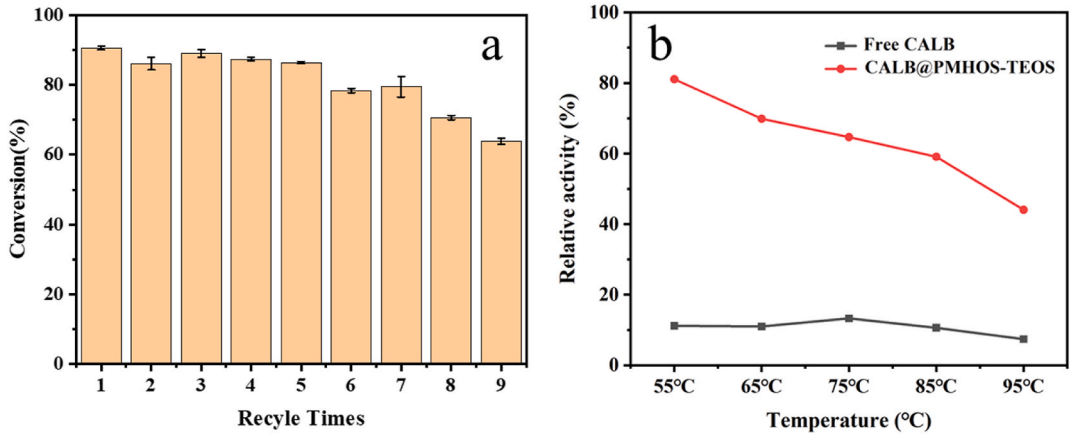

Fig. 5. Reusability and Thermal stability study. (a) Graph of Conversion percentage versus Recycle times to illustrate the reusability of CALB@PMHOS-TEOS evaluated by cyclic synthesis of ethyl hexanoate in deionized water (41.1 wt%), enzyme (3%), hexanoic acid and anhydrous ethanol molar ratio (1:2) in a water bath (35 °C, 200 rpm) for 2 h. (b) Graph of Relative Activity versus Temperature to illustrate the Thermal stability of free CALB and CALB@PMHOS-TEOS at varying temperatures from 55 °C to 95 °C.

Table 1
Enzymatic synthesis of a series of alcoholic flavor esters.

Flavor Ester	Acyl donor	Main flavor property	2 h conversion (%)	Catalytic efficiency (μmol/g·min)
Ethyl valerate	Pentanoic acid	Apple	77.2 ± 1.4	1111.2
Ethyl hexanoate	Hexanoic acid	Distilled wine	90.6 ± 0.6	1198.4
Ethyl heptanoate	Heptanoic acid	Pineapple	91.2 ± 1.7	1134.0
Ethyl octanoate	Octanoic acid	Fruity	93.2 ± 0.9	1084.9
Ethyl nonanoate	Nonanoic acid	Rose	94.9 ± 1.4	1054.4
Ethyl decanoate	Decanoic acid	Copra	99.9 ± 0.5	1052.7
Ethyl laurate	Lauric acid	Floral and fruity	98.9 ± 0.8	943.8

decanoate, and ethyl laurate, with corresponding conversions ranging from 77.2 ± 1.4 % to 99.9 ± 0.5%; these esters demonstrate high conversion and catalytic efficiency. In this study, the results of the hexanoic acid conversion were compared with reported in previous literature (Table 2). For instance, Mulay & Rathod's results showed that when the amount of lipase Amberlyst-15 added was 11%, the conversion rate of ethyl hexanoate was only 83.9%. (Mulay & Rathod, 2022). Although Han et al. achieved the highest conversion of 98.2% with the catalytic efficiency of *Saccharomyces cerevisiae* whole-cells reaching 909 μmol/g·min, the use of n-heptane as reaction solvent necessitated further separation and purification (Han et al., 2009). Similarly, Musa et al. (2018) reported the 80% conversion rate for the enzymatic synthesis of ethyl hexanoate catalyzed by AMS8, using toluene as the organic reagent. In addition, Wang, Wang, Zhang, and Chen (2019) utilized immobilized lipase CALB to catalyze the synthesis of hexyl hexanoate with a high conversion rate of 96.5% in a Pickering emulsion system. However, the main issues included the extended reaction time of 24 h and the addition of heptane. Compared to the literature mentioned above, the self-made immobilized lipase CALB@PMHOS-TEOS achieved a comparable ethyl hexanoate conversion rate of 90.6% without the need for organic solvents. This demonstrates significant advantages for sustainable production, particularly in food-related areas. Additionally, the high catalytic efficiency of 1198.4 μmol/g·min exhibited by CALB@PMHOS-TEOS further emphasizes its potential for enzymatic production.

3.7. Molecular docking analysis

The conversion of fatty acids is accompanied by a gradual increase in chain length. In order to gain insights into the interactions between lipase and small molecule fatty acids, a molecular docking model was developed to simulate and elucidate the strength of their binding affinity. In this study, the active site of lipase CALB comprises a catalytic triad (Ser 105, His 224, Asp 187), which is attributed to a charge transfer mechanism. Two amino acid residues, Gln 106 and Thr 40, contribute to stable hydrogen bonds with oxygen-negative ions (Gu et al., 2019). The investigation into the relationship between fatty acids and lipase CALB conversion percentage considered amino acid residues as the active center pocket in the molecular docking model. Fig. 6 shows the binding of various fatty acids to lipase within the active center pocket based on the molecular docking model. The effective binding of all the fatty acids to the pocket indicates a strong form complementarity (Zhang et al.,

Table 2
Comparison of enzymatic synthesis of ethyl hexanoate.

Lipase	Hexanoic acid (μmol)	Lipase addition (mg)	Time (h)	Temperature (°C)	Solvent	Conversion (%)	Catalytic efficiency (μmol/g·min)	References
Amberlyst-15	119.1×10^3	2790	2.2	60	–	83.9	275.5	Mulay and Rathod (2022)
CALB-displaying Saccharomyces cerevisiae whole-cells	200×10^3	300	12	40	n-heptane	98.2	909	Han et al. (2009)
AMS8	25×10^3	729	2	20	toluene	80	821	(Musa et al., 2018)
CALB@PMHOS-TEOS	10×10^3	63	2	35	–	90.6	1198.4	This study

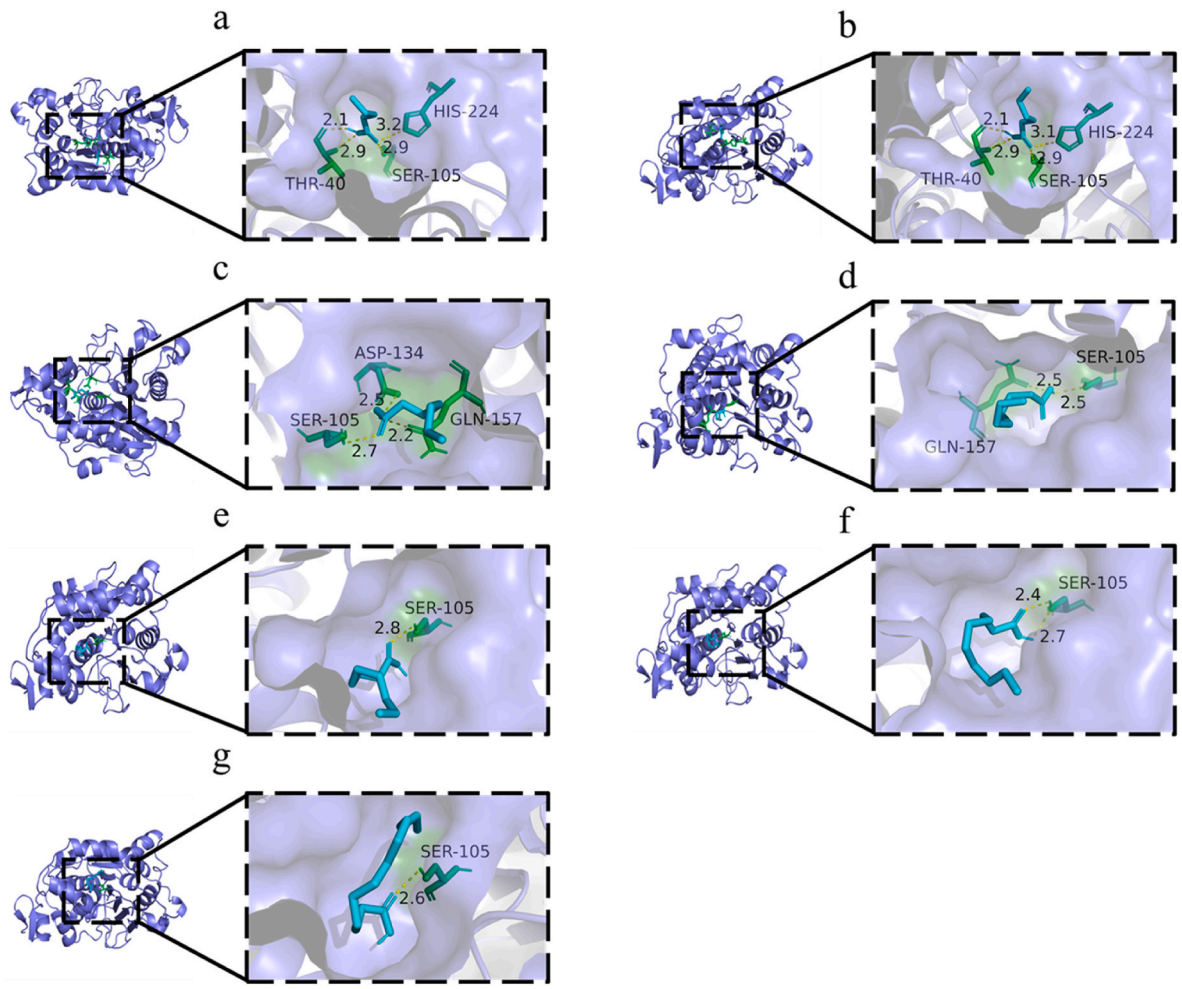

Fig. 6. Schematic representation of the binding process of (a) pentanoic acid, (b) hexanoic acid, (c) heptanoic acid, (d) octanoic acid, (e) nonanoic acid, (f) decanoic acid, and (g) lauric acid to lipase CALB.

2022). Hydrogen bonding and hydrophobic interactions are the primary mechanisms by which lipase binds to fatty acids. In particular, hydrogen bonds formed at short distances are essential for maintaining the stability of the secondary structures of proteins (Hung, Kuo, Lee, & Chiang, 2021). Despite variations in the types of fatty acids and their respective binding sites, the results reveal that they all engage in hydrogen bonding interactions with amino acid residues (Ser 105) in the active site. This phenomenon arises from the nucleophilic nature of Ser 105, which has a specific affinity for water molecules in the biphasic system (Li & Zhang, 2020). It is shown through Fig. S3I that fatty acids interact with nearby amino acid residues in addition to binding to the catalytic triad and oxygen anion cavity residues. In the enzymatic reactions between valeric acid and lipase, interactions primarily involved five amino acid residues, including Leu 278, Ile 189, Ile 285, Ser 105, and Thr 40 as illustrated in Fig. S3a. Similarly, the amino acid residues that affect the bonding of lipases with other fatty acids were also illustrated (Figs. S3b–g). The main forces involved in fatty acid binding to lipase, including hydrogen bonding and hydrophobic interactions, are revealed in Fig. S3II. Together with hydrogen bonding and hydrophobic interactions, π-σ and π-alkyl interactions, weak interactions between the oxygen and ring systems, respectively, also occur during the docking of lauric acid with lipase.

Table 3 shows the specific binding energies between each fatty acid with lipase CALB under the same conditions. The docking binding energies were calculated in the order of increasing magnitude as follows: ethyl valerate (−4.4 kJ/mol), ethyl hexanoate (−4.6 kJ/mol), ethyl heptanoate (−4.7 kJ/mol), ethyl octanoate (−4.7 kJ/mol), ethyl nonanoate (−4.9 kJ/mol), ethyl decanoate (−5.0 kJ/mol), ethyl laurate (−5.4 kJ/mol). It can be seen that the binding energy gradually increase with increasing length of the carbon chains of fatty acids due to the increased affinity between the fatty acids and the lipase CALB. Furthermore, the selectivity of the active pocket of CALB also increases with longer fatty acid carbon chain length, in good agreement with the observed trend in the conversion rate change (Zhang et al., 2022).

Table 3
The binding energy of lipase CALB -fatty acid complexes.

Complex	Binding energy (kcal/mol)	RMSD	Conversion (%)
Ethyl valerate	−4.4	0.958	77.2 ± 1.4
Ethyl hexanoate	−4.6	2.247	90.6 ± 0.6
Ethyl heptanoate	−4.7	1.117	91.2 ± 1.7
Ethyl octanoate	−4.7	1.201	93.2 ± 0.9
Ethyl nonanoate	−4.9	1.792	94.9 ± 1.4
Ethyl decanoate	−5.0	2.347	99.9 ± 0.5
Ethyl laurate	−5.4	2.750	98.9 ± 0.8

4. Conclusions

In this paper, a new lipase microarray CALB@PMHOS-TEOS was prepared by immobilizing lipase CALB on a surfactant-free hydrophobic mesoporous material, for the synthesis of ethyl caproate flavored ester using caproic acid and ethanol. The conversion of caproic acid was as high as 93.5 ± 0.5 % in a 2 h reaction time. The CALB@PMHOS-TEOS

enzyme maintained a high yield after 9 cycles of repeated use and exhibited remarkable thermal stability. The newly developed, highly efficient, solvent-free, and recyclable reaction system for the biocatalytic synthesis of alcoholic flavor esters holds great potential for applications in the food and cosmetic, providing a way for further development.

CRediT authorship contribution statement

Yiran Bian: Writing – original draft, Methodology, Investigation. **Yi Zhang:** Writing – review & editing, Writing – original draft, Methodology. **Taosuo Wang:** Validation. **Chuang Yang:** Visualization. **Zhiming Feng:** Writing – review & editing, Formal analysis. **Kheng-Lim Goh:** Writing – review & editing, Formal analysis. **Yibin Zhou:** Writing – review & editing, Visualization. **Mingming Zheng:** Writing – review & editing, Supervision, Funding acquisition, Conceptualization.

Declaration of competing interest

The authors declare that they have no known competing financial interests or personal relationships that could have appeared to influence the work reported in this paper.

Data availability

Data will be made available on request.

Acknowledgments

This study was supported by National Key Research and Development Project of China (2021YFD2100303), National Natural Science Foundation of China (32272271, 32302021), Hubei Province Natural Science Foundation of China (2023AFB324), Major Project of Hubei Hongshan Laboratory (2022hszd002), Central Public-interest Scientific Institution Basal Research Fund (No. 1610172022014), Anhui Province Key Research and Development Program Project (2023n06020039) and Anhui Province Science and Technology Major Special Project (202003b06020002).

Appendix A. Supplementary data

Supplementary data to this article can be found online at https://doi.org/10.1016/j.lwt.2024.116206.

References

Al-Lolage, F. A., Meneghello, M., Ma, S., Ludwig, R., & Bartlett, P. N. (2017). A Flexible method for the stable, covalent immobilization of enzymes at Electrode surfaces. *Chemelectrochem, 4*(6), 1528–1534. https://doi.org/10.1002/celc.201700135

Alvarez-Macarie, E., & Baratti, J. (2000). Short chain flavour ester synthesis by a new esterase from Bacillus licheniformis. *Journal of Molecular Catalysis B: Enzymatic, 10*(4), 377–383. https://doi.org/10.1016/S1381-1177(99)00109-5

Badgujar, K. C., & Bhanage, B. M. (2014). Application of lipase immobilized on the biocompatible ternary blend polymer matrix for synthesis of citronellyl acetate in non-aqueous media: Kinetic modelling study. *Enzyme and Microbial Technology, 57*, 16–25. https://doi.org/10.1016/j.enzmictec.2014.01.006

Bai, Y., & Wu, W. (2022). The neutral protease immobilization: Physical characterization of sodium alginate-chitosan gel beads. *Applied Biochemistry and Biotechnology, 194*(5), 2269–2283. https://doi.org/10.1007/s12010-021-03773-9

Bansode, S. R., & Rathod, V. K. (2014). Ultrasound assisted lipase catalysed synthesis of isoamyl butyrate. *Process Biochemistry, 49*(8), 1297–1303. https://doi.org/10.1016/j.procbio.2014.04.018

Bhavsar, K. V., & Yadav, G. D. (2018). Process intensification by microwave irradiation in immobilized-lipase catalysis in solvent-free synthesis of ethyl valerate. *Molecular Catalysis, 461*, 34–39. https://doi.org/10.1016/j.mcat.2018.09.019

Chen, J., Zhang, Y., Zhong, H., Zhu, H., Wang, H., Goh, K.-L., et al. (2023). Efficient and sustainable preparation of cinnamic acid flavor esters by immobilized lipase microarray. *Lebensmittel-Wissenschaft & Technologie, 173*, Article 114322. https://doi.org/10.1016/j.lwt.2022.114322

Çıtak, A., Erdem, B., Erdem, S., & Öksüzoğlu, R. M. (2012). Synthesis, characterization and catalytic behavior of functionalized mesoporous SBA-15 with various organosilanes. *Journal of Colloid and Interface Science, 369*(1), 160–163. https://doi.org/10.1016/j.jcis.2011.11.070

de Barros, D. P. C., Fonseca, L. P., Fernandes, P., Cabral, J. M. S., & Mojovic, L. (2009). Biosynthesis of ethyl caproate and other short ethyl esters catalyzed by cutinase in organic solvent. *Journal of Molecular Catalysis B: Enzymatic, 60*(3), 178–185. https://doi.org/10.1016/j.molcatb.2009.05.004

Dong, Z., Liu, Z., Shi, J., Tang, H., Xiang, X., Huang, F., et al. (2019). Carbon nanoparticle-stabilized pickering emulsion as a sustainable and high-performance interfacial catalysis platform for enzymatic esterification/transesterification. *ACS Sustainable Chemistry & Engineering, 7*(8), 7619–7629. https://doi.org/10.1021/acssuschemeng.8b05908

Elgharbawy, A. A., Riyadi, F. A., Alam, M. Z., & Moniruzzaman, M. (2018). Ionic liquids as a potential solvent for lipase-catalysed reactions: A review. *Journal of Molecular Liquids, 251*, 150–166. https://doi.org/10.1016/j.molliq.2017.12.050

Foresti, M. L., & Ferreira, M. L. (2005). Solvent-free ethyl oleate synthesis mediated by lipase from Candida antarctica B adsorbed on polypropylene powder. *Catalysis Today, 107–108*, 23–30. https://doi.org/10.1016/j.cattod.2005.07.053

Gawas, S., Lokanath, N., & Rathod, V. (2018). Optimization of enzymatic synthesis of ethyl hexanoate in a solvent free system using response surface methodology (RSM). *Biocatalysis, 4*, 14–26. https://doi.org/10.1515/boca-2018-0002

Ghanem, A., & Aboul-Enein, H. Y. (2004). Lipase-mediated chiral resolution of racemates in organic solvents. *Tetrahedron: Asymmetry, 15*(21), 3331–3351. https://doi.org/10.1016/j.tetasy.2004.09.019

Gu, B., E Hu, Z., Yang, Z.-J., Li, J., Zhou, Z.-W., Wang, N., et al. (2019). Probing the mechanism of CAL-B-catalyzed aza-michael addition of aniline compounds with acrylates using mutation and molecular docking simulations. *ChemistrySelect, 4*(13), 3848–3854. https://doi.org/10.1002/slct.201900112

Han, S.-Y., Pan, Z.-Y., Huang, D.-F., Ueda, M., Wang, X.-N., & Lin, Y. (2009). Highly efficient synthesis of ethyl hexanoate catalyzed by CALB-displaying Saccharomyces cerevisiae whole-cells in non-aqueous phase. *Journal of Molecular Catalysis B: Enzymatic, 59*(1), 168–172. https://doi.org/10.1016/j.molcatb.2009.02.007

Hari Krishna, S., Divakar, S., Prapulla, S. G., & Karanth, N. G. (2001). Enzymatic synthesis of isoamyl acetate using immobilized lipase from Rhizomucor miehei. *Journal of Biotechnology, 87*(3), 193–201. https://doi.org/10.1016/S0168-1656(00)00432-6

Hung, C.-L., Kuo, Y.-H., Lee, S. W., & Chiang, Y.-W. (2021). Protein stability depends critically on the surface hydrogen-bonding network: A case study of bid protein. *The Journal of Physical Chemistry B, 125*(30), 8373–8382. https://doi.org/10.1021/acs.jpcb.1c03245

Jaiswal, K. S., & Rathod, V. K. (2018). Acoustic cavitation promoted lipase catalysed synthesis of isobutyl propionate in solvent free system: Optimization and kinetic studies. *Ultrasonics Sonochemistry, 40*, 727–735. https://doi.org/10.1016/j.ultsonch.2017.07.026

Jaiswal, K. S., & Rathod, V. K. (2022). Process intensification of enzymatic synthesis of flavor esters: A review. *The Chemical Record, 22*(3), Article e202100213. https://doi.org/10.1002/tcr.202100213

Jiang, H., Li, Y., Hong, L., & Ngai, T. (2018). Submicron inverse pickering emulsions for highly efficient and recyclable enzymatic catalysis. *Chemistry - An Asian Journal, 13*(22), 3533–3539. https://doi.org/10.1002/asia.201800853

Kuang, L., Zhang, Q., Li, J., & Tian, H. (2020). Preparation of lipase–electrospun SiO2 nanofiber membrane bioreactors and their targeted catalytic ability at the macroscopic oil–water interface. *Journal of Agricultural and Food Chemistry, 68*(31), 8362–8369. https://doi.org/10.1021/acs.jafc.0c02801

Kumar, A., Dhar, K., Kanwar, S. S., & Arora, P. K. (2016). Lipase catalysis in organic solvents: Advantages and applications. *Biological Procedures Online, 18*(1), 2. https://doi.org/10.1186/s12575-016-0033-2

Laane, C., Boeren, S., Vos, K., & Veeger, C. (2009). Rules for optimization of biocatalysis in organic solvents. *Biotechnology and Bioengineering, 102*(1), 1–8. https://doi.org/10.1002/bit.22209

Lai, Y., Li, D., Liu, T., Wan, C., Zhang, Y., Zhang, Y., et al. (2023). Preparation of functional oils rich in diverse medium and long-chain triacylglycerols based on a broadly applicable solvent-free enzymatic strategy. *Food Research International, 164*, Article 112338. https://doi.org/10.1016/j.foodres.2022.112338

Lammirato, C., Miltner, A., & Kaestner, M. (2011). Effects of wood char and activated carbon on the hydrolysis of cellobiose by β-glucosidase from Aspergillus Niger. *Soil Biology & Biochemistry - SOIL BIOL BIOCHEM, 43*, 1936–1942. https://doi.org/10.1016/j.soilbio.2011.05.021

Li, X., & Zhang, J. (2020). Study on lipase-catalyzed hydrolysis of olive oil at oil-water interface. *Tenside Surfactants Detergents, 57*(3), 211–221. https://doi.org/10.3139/113.110681

Luan, B., & Zhou, R. (2017). A novel self-activation mechanism of Candida Antarctica lipase B. *Physical Chemistry Chemical Physics, 19*(24), 15709–15714. https://doi.org/10.1039/C7CP02198D

Monteiro, R. R. C., Neto, D. M. A., Fechine, P. B. A., Lopes, A. A. S., Gonçalves, L. R. B., dos Santos, J. C. S., et al. (2019). Ethyl butyrate synthesis catalyzed by lipases A and B from Candida Antarctica immobilized onto magnetic nanoparticles. Improvement of biocatalysts' performance under ultrasonic irradiation. *International Journal of Molecular Sciences, 20*(22). https://doi.org/10.3390/ijms20225807

Mulay, A., & Rathod, V. K. (2022). Ultrasound-assisted synthesis of ethyl hexanoate using heterogeneous catalyst: Optimization using Box-Behnken design. *Journal of the Indian Chemical Society, 99*(8), Article 100573. https://doi.org/10.1016/j.jics.2022.100573

Musa, N., Latip, W., Abd Rahman, R. N., Salleh, A. B., & Mohamad Ali, M. S. (2018). Immobilization of an antarctic Pseudomonas AMS8 lipase for low temperature ethyl hexanoate synthesis. *Catalysts, 8*(6). https://doi.org/10.3390/catal8060234

Nagappan, S., & Ha, C.-S. (2017). In-situ addition of graphene oxide for improving the thermal stability of superhydrophobic hybrid materials. *Polymer, 116*, 412–422. https://doi.org/10.1016/j.polymer.2016.12.072

Nagappan, S., Lee, D. B., Seo, D. J., Park, S. S., & Ha, C.-S. (2015). Superhydrophobic mesoporous material as a pH-sensitive organic dye adsorbent. *Journal of Industrial and Engineering Chemistry, 22*, 288–295. https://doi.org/10.1016/j.jiec.2014.07.022

Naseer, S., Ouyang, J., Chen, X., Pu, S., Guo, Y., Zhang, X., et al. (2020). Immobilization of β-glucosidase by self-catalysis and compared to crosslinking with glutaraldehyde. *International Journal of Biological Macromolecules, 154*, 1490–1495. https://doi.org/10.1016/j.ijbiomac.2019.11.030

Pélisson, C.-H., Nakanishi, T., Zhu, Y., Morisato, K., Kamei, T., Maeno, A., et al. (2017). Grafted polymethylhydrosiloxane on hierarchically porous silica monoliths: A new path to monolith-supported palladium nanoparticles for continuous flow catalysis applications. *ACS Applied Materials & Interfaces, 9*(1), 406–412. https://doi.org/10.1021/acsami.6b12653

Qin, X., Zhong, J., & Wang, Y. (2021). A mutant T1 lipase homology modeling, and its molecular docking and molecular dynamics simulation with fatty acids. *Journal of Biotechnology, 337*, 24–34. https://doi.org/10.1016/j.jbiotec.2021.06.024

Romero, M. D., Calvo, L., Alba, C., Daneshfar, A., & Ghaziaskar, H. S. (2005). Enzymatic synthesis of isoamyl acetate with immobilized Candida Antarctica lipase in n-hexane. *Enzyme and Microbial Technology, 37*(1), 42–48. https://doi.org/10.1016/j.enzmictec.2004.12.033

Sa, A. G. A., Meneses, A. C.d., Araújo, P. H. H.d., & Oliveira, D.d. (2017). A review on enzymatic synthesis of aromatic esters used as flavor ingredients for food, cosmetics and pharmaceuticals industries. *Trends in Food Science & Technology, 69*, 95–105. https://doi.org/10.1016/j.tifs.2017.09.004

Sun, T., Dong, Z., Wang, J., Huang, F.-H., & Zheng, M.-M. (2020). Ultrasound-assisted interfacial immobilization of lipase on hollow mesoporous silica spheres in a pickering emulsion system: A hyperactive and sustainable biocatalyst. *ACS Sustainable Chemistry & Engineering, 8*(46), 17280–17290. https://doi.org/10.1021/acssuschemeng.0c06271

Vasilescu, C., Todea, A., Nan, A., Circu, M., Turcu, R., Benea, I.-C., et al. (2019). Enzymatic synthesis of short-chain flavor esters from natural sources using tailored magnetic biocatalysts. *Food Chemistry, 296*, 1–8. https://doi.org/10.1016/j.foodchem.2019.05.179

Wang, L., Ding, W., & Sun, Y. (2016). The preparation and application of mesoporous materials for energy storage. *Materials Research Bulletin, 83*, 230–249. https://doi.org/10.1016/j.materresbull.2016.06.008

Wang, Z., van Oers, M. C. M., Rutjes, F. P. J. T., & van Hest, J. C. M. (2012). Polymersome colloidosomes for enzyme catalysis in a biphasic system. *Angewandte Chemie International Edition, 51*(43), 10746–10750. https://doi.org/10.1002/anie.201206555

Wang, M., Wang, M., Zhang, S., & Chen, J. (2019). Pickering gel emulsion stabilized by enzyme immobilized polymeric nanoparticles: A robust and recyclable biocatalyst system for biphasic catalysis. *Reaction Chemistry & Engineering, 4*(8), 1459–1465. https://doi.org/10.1039/C9RE00158A

Wang, H., Zhang, Y., Yue, W., Liang, J., & Su, W. (2022). Application of magnetic field (MF) as an effective method to improve the activity of immobilized Candida Antarctica lipase B (CALB). *Catalysis Science and Technology, 12*(17), 5315–5324. https://doi.org/10.1039/D2CY00628F

Xu, L.-J., Yang, T., Wang, J., Huang, F.-H., & Zheng, M.-M. (2021). Immobilized lipase based on hollow mesoporous silicon spheres for efficient enzymatic synthesis of resveratrol ester derivatives. *Journal of Agricultural and Food Chemistry, 69*(32), 9067–9075. https://doi.org/10.1021/acs.jafc.0c07501

Yang, D., Xu, Y., Wu, D., Sun, Y., Zhu, H., & Deng, F. (2007). Super hydrophobic mesoporous silica with anchored methyl groups on the surface by a one-step synthesis without surfactant template. *Journal of Physical Chemistry C, 111*(2), 999–1004. https://doi.org/10.1021/jp065815u

Zhai, S.-R., Song, Y., Zhai, B., An, Q.-D., & Ha, C.-S. (2012). One-pot synthesis of hybrid mesoporous xerogels starting with linear polymethylhydrosiloxane and bridged bis-(trimethoxysilyl)ethane. *Microporous and Mesoporous Materials, 163*, 178–185. https://doi.org/10.1016/j.micromeso.2012.07.022

Zhang, T., Zhang, Y., Deng, C., Zhong, H., Gu, T., Goh, K.-L., et al. (2022). Green and efficient synthesis of highly liposoluble and antioxidant L-ascorbyl esters by immobilized lipases. *Journal of Cleaner Production, 379*, Article 134772. https://doi.org/10.1016/j.jclepro.2022.134772

Zheng, M., Mao, L., Huang, F., Xiang, X., Deng, Q., & Feng, Y. (2015). A mixed-function-grafted magnetic mesoporous hollow silica microsphere immobilized lipase strategy for ultrafast transesterification in a solvent-free system. *RSC Advances, 5*(54), 43074–43080. https://doi.org/10.1039/C5RA05611J